Individually addressable vertically aligned carbon nanofiber-based electrochemical probes

M. A. Guillorn,[a] T. E. McKnight, A. Melechko, V. I. Merkulov, P. F. Britt, D. W. Austin, D. H. Lowndes, and M. L. Simpson
Molecular-Scale Engineering and Nanoscale Technologies Research Group, Oak Ridge National Laboratory, Oak Ridge, Tennessee 37831, and University of Tennessee, Knoxville, Tennessee 37996

(Received 19 October 2001; accepted for publication 30 November 2001)

In this paper we present the fabrication and initial testing results of high aspect ratio vertically aligned carbon nanofiber (VACNF)-based electrochemical probes. Electron beam lithography was used to define the catalytic growth sites of the VACNFs. Following catalyst deposition, VACNF were grown using a plasma enhanced chemical vapor deposition process. Photolithography was performed to realize interconnect structures. These probes were passivated with a thin layer of SiO_2, which was then removed from the tips of the VACNF, rendering them electrochemically active. We have investigated the functionality of completed devices using cyclic voltammetry (CV) of ruthenium hexammine trichloride, a highly reversible, outer sphere redox system. The faradaic current obtained during CV potential sweeps shows clear oxidation and reduction peaks at magnitudes that correspond well with the geometry of these nanoscale electrochemical probes. Due to the size and the site-specific directed synthesis of the VACNFs, these probes are ideally suited for characterizing electrochemical phenomena with an unprecedented degree of spatial resolution.
[DOI: 10.1063/1.1448671]

I. INTRODUCTION

An enormous body of knowledge has been accumulated about intracellular processes using the classical techniques of biochemistry, in which processes and structures are analyzed in subcellular fractions derived from the lysate of disrupted cells. While these techniques are of unquestionable value, they are destructive and provide a single data point in time and very little in the way of spatial resolution. Nondestructive time- and spatially resolved analysis techniques could add a great deal to the understanding of cellular processes that take place within the highly organized and ordered environment of the *living* cell. While advances in molecular biology and imaging technology are providing enormous insight into the genetic code and cellular structure, our ability to monitor detailed, ongoing processes within and around living cells remains extremely limited. This limitation is largely technological: our current research instruments are simply not on the same scale as the cell and its components.

Microelectrophysiological electrochemical measurements and electroanalytical detection techniques, performed using ultramicroelectrodes ($<50\ \mu$m), are emerging as promising avenues for the interrogation and monitoring of chemical dynamics at the single cell level. The promise of these electrodes lies in their fast response times ($\sim$ms), high mass sensitivity (zeptomole, i.e., 100–1000 molecules), small size, large linear dynamic range, and because molecules of interest can be followed without the need for chemical derivitization, as is necessary with fluorescent probe techniques. Carbon fiber microelectrodes, fabricated by placing microscale carbon fiber elements into glass capillary tubes, have become the electrode of choice for many extra- and intracellular measurement applications. For easily oxidizable substances (i.e., catecholamines,[1] indoleamines,[2] oxygen,[3] and doxorubicin[4]) the native carbon electrode surface is sufficient for electrochemical analysis, and these substances have been readily detected in or near the surface of single cells.

While single element, pulled capillary carbon fiber microelectrodes will continue to provide enormous insight into cellular-scale phenomena, a method for penetrating cells with multiple electrochemical probes would greatly facilitate our understanding of intracellular processes by allowing us to monitor various phenomena in real time. As with any probe array, issues such as signal leakage and electrical isolation must be addressed. Moreover, in intracellular applications, probes must possess a small diameter and a high-aspect ratio to provide a minimally invasive penetration into the cell, reducing the physiological impact of probe insertion, and thereby improving cell viability during experimentation.

Recent research performed by our group in the fabrication of vertically aligned carbon nanofiber (VACNF) arrays and devices[5–8] offers the opportunity to design high aspect ratio probes that function at a size scale ideal for probing at the cellular level. Here we present a robust and scalable process for fabricating high aspect ratio VACNF-based probes that can be used to probe a variety of electrochemical events with high spatial resolution. We have demonstrated the performance of these probes by showing that they can drive an electrochemical reaction localized to the probe tip. This was accomplished by examining the faradaic current of a single probe device during cyclic voltammetry.

[a]Corresponding author; electronic mail: guillornma@ornl.gov

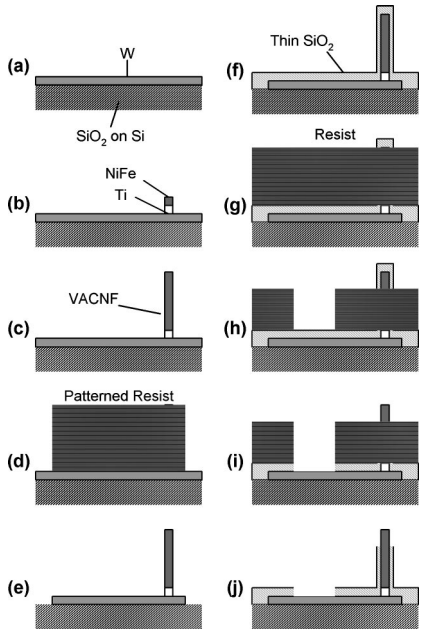

FIG. 1. Fabrication process outline for VACNF-based electrochemical probes.

II. FABRICATION

The fabrication process used in this work is summarized in Fig. 1. The substrates used throughout this work were 3-in *n*-type low resistivity Si wafers that had been thermally oxidized to form a 1200 Å passivating layer of SiO_2. A 500 Å thick layer of W was deposited onto the wafer by rf sputtering in a vacuum chamber with a base pressure of 10^{-6} Torr [refer to Fig. 1(a)]. Electron beam lithography (EBL) was performed to define the catalyst sites as described in previous work.[6] The exposed pattern consisted of a 2×2 array of 100 nm dots and alignment marks for subsequent lithography steps. The wafers were exposed with a 3×3 array of this pattern forming nine discrete die per wafer, with 15 mm separation between each die.

The exposures were developed in a solution of MIBK: Isopropanol 1:3 for 1 min, rinsed in isopropanol and blown dry with N_2. Following inspection in an optical microscope, the patterns were metallized using a liftoff technique. One hundred Å of Ti followed by 100 Å of NiFe alloy (50/50) was deposited by electron gun physical vapor deposition (PVD) onto the wafers in a vacuum chamber with a base pressure of 10^{-6} Torr. The coated wafers were immersed in beakers containing acetone for 1 h. The acetone dissolved the unexposed resist, removing the metal from the unpatterned areas of the substrate, leaving behind a positive metal image of the exposed pattern [refer to Fig. 1(b)]. To ensure that the surface of the substrate remained free from any metallic debris, the substrates were kept in the beakers of acetone and placed in an ultrasonic agitator for 30 s. The substrates were then removed from the acetone while being sprayed with isopropanol and then blown dry with N_2.

DC plasma enhanced chemical vapor deposition (PECVD) growth of VACNFs was performed as described in previous works[6,8] [refer to Fig. 1(c)]. The VACNFs produced for this work were conical in shape and featured, on average, a base diameter of 200 nm, a height of 1 μm, and a tip radius of curvature of 20 nm.

The wafers were spin coated in 1 μm of photoresist (Olin, OiR 620-7i), and the pattern for the probe interconnects was exposed using a brightfield mask. The exposures were performed using a GCA Autostep200 $5\times$ reduction stepper. This tool is capable of exposing patterns with less than 50 nm of overlay mismatch between pre-existing EBL defined features as demonstrated in previous work.[6] The wafers were subjected to a post-exposure bake at 115 °C for 1 min and then developed in a standard aqueous developer (Shipley, CD-26) for 1 min, rinsed in deionized water and then blown dry in N_2 [refer to Fig. 1(d)].

To transfer the electrode pattern into the W layer, the wafers were placed in a reactive ion etch (RIE) chamber and subjected to an RF CF_4:SF_6 (40 sccm: 10 sccm) plasma for 2 min. The chamber was operated at a pressure of 40 mTorr with a plasma power density of 0.2 W/cm^2. These conditions were found to etch W at a rate of roughly 30 nm/min. Following the etch, the wafers were removed from the chamber and immersed in acetone to strip away the remaining photoresist [refer to Fig. 1(e)].

To passivate the sidewalls of the fibers and the surface of the electrode interconnects a 50-nm-thick layer of SiO_2 was deposited onto the substrates using a silane-based rf PECVD process. This process created a uniform oxide covering over the VACNF and interconnects [refer to Fig. 1(f)]. To complete the probes, a final layer of photoresist was spun onto the substrates as described above [refer to Fig. 1(g)]. A darkfield mask with an array of rectangles aligned to the bonding pads of the interconnects was then exposed and developed as described above [refer to Fig. 1(h)]. The wafers were then placed in an RIE chamber and etched in an O_2 plasma (30 sccm) for 1 min followed by a CHF_3:O_2 (30 sccm:1 sccm) plasma for 2 min. Both plasmas were operated at a chamber pressure of 50 mTorr and a power density of 0.25 W/cm^2. The O_2 etch served to remove resist from the tips of the passivated fibers and any residual resist from the exposed pattern of the bonding pads. The CHF_3:O_2 etch removed the SiO_2 layer from the fiber tips and the bonding pads, allowing these two sites to become electrically active [refer to Fig. 1(i)]. The resist was then stripped from the wafers by immersion in acetone for 1 h, ultrasonic agitation for 30 s, and a short exposure to an O_2 plasma [refer to Fig. 1(j)] for 10 s.

III. RESULTS OF THE FABRICATION PROCESS

Figure 2 shows a scanning electron microscope (SEM) micrograph of a VACNF on a W electrode following the interconnect pattern transfer step. Using a manual electrical probe station and an HP 4156 source measure unit, the electrical isolation of the interconnects was investigated by examining the current versus voltage ($I-V$) response between each interconnect and the substrate. The leakage current was found to be in the subpicoampere regime and was assumed to be below the sensitivity limits of our measurement apparatus. The electrical continuity of the leads was inspected

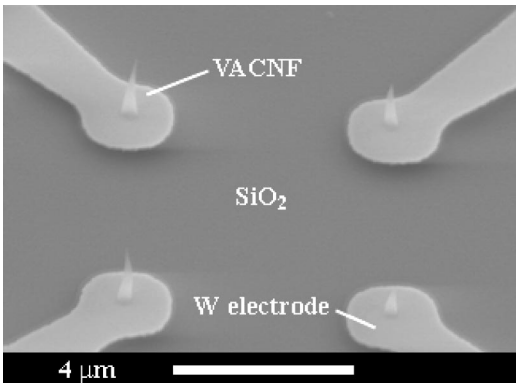

FIG. 2. SEM micrograph of four VACNF probes on individual W pads taken at 45° from normal incidence.

visually in an SEM to ensure that no obvious defects in the metallization had occurred during processing.

An SEM micrograph of a passivated VACNF probe device is shown in Fig. 3. This image was taken at an accelerating voltage of 10 kV to allow penetration of the electron beam through the thin passivating oxide to the underlying carbon and W layers. Figure 4 shows a close up of the probe device shown in Fig. 3. From this image it is clear that a contrast difference exists between the apex of the probe and the rest of the probe device corresponding to a bare carbon surface at the tip. In order to further investigate whether the oxide removal process was successful at the tip, the passivated VACNFs of completed devices were removed from the substrate and examined using an SEM equipped with a low voltage transmitted electron detector. A micrograph from this study is shown in Fig. 5 and reveals that the VACNF tip is free of oxide while the VACNF body remains passivated.

For these nanoscale probes to be useful, it was extremely important that the W interconnects did not contribute to electron transfer to the electrolyte solution. Therefore, the passivation oxide had to be pinhole free. To evaluate the quality of the oxide layer, Au was electrodeposited onto the structures using a commercial electroplating solution (Technic, Inc., Orotherm HT). Twenty microliters of the plating solution was applied directly to the array region of a single device. A Hewlett Packard 4156 source measurement unit was used to apply −1.5 V to the contact pad of an individual element of the fiber array with respect to a 20 mil Pt wire used as the reference electrode. Electroplating was performed on both passivated and nonpassivated (bare W and carbon fibers) substrates. The structures were then dried, baked on a hotplate for 15 min at 150 °C and then examined in an SEM equipped with a backscattered electron detector and an energy dispersive x-ray detector. Using a combination of these detectors on several samples it was found that, on average, passivated devices did not show any presence of Au on the interconnect structures while unpassivated devices featured gold depositions uniformly at all W and carbon sites located under the plating solution droplet. Au clusters on the sides of the interconnects were found on a small number of passivated devices (less than 25%). Typically, the electrochemical activity of the passivated structures appeared restricted to the bare carbon fiber tips where large Au clusters,

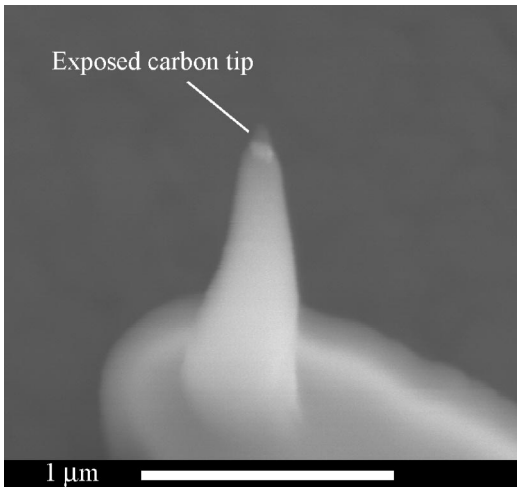

FIG. 4. High magnification SEM micrograph of the probe tip of the device shown in Fig. 3 taken at 45° from normal incidence. This image was taken at an accelerating voltage of 10 kV and shows a clear contrast difference between the apex of the probe and the body of the VACNF. This contrast change corresponds to a bare carbon surface and an oxide passivated carbon surface.

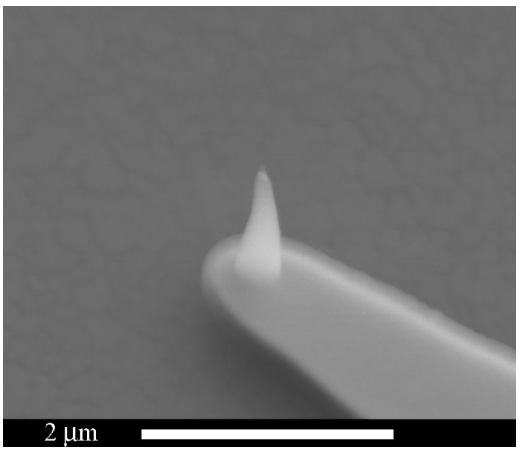

FIG. 3. SEM micrograph of a completed VACNF-based electrochemical probe device taken at 45° from normal incidence.

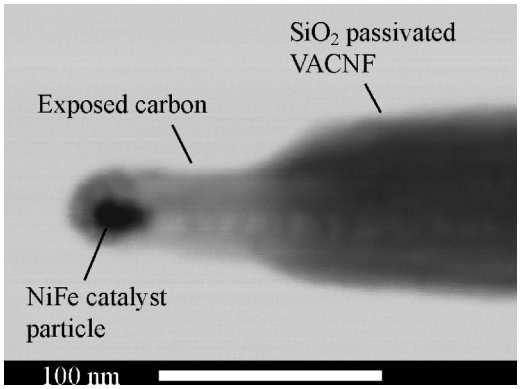

FIG. 5. Transmission mode SEM image of a VACNF-based probe tip that was removed from the W interconnect. This image clearly shows that this process is capable of selectively removing oxide from the VACNF tip while leaving the fiber body encased.

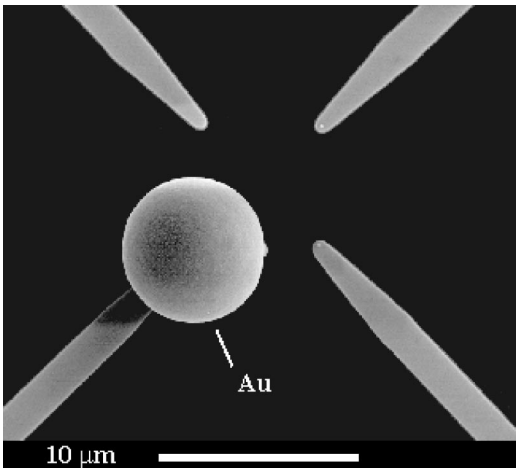

FIG. 6. SEM micrograph of a VACNF array following electrodeposition of Au on the lower left probe taken at normal incidence. The presence of the large Au ball centered at the location of the fiber demonstrates that the probes are electrochemically active while the lack of Au on the interconnect structures shows that the passivating oxide is free of pinhole defects.

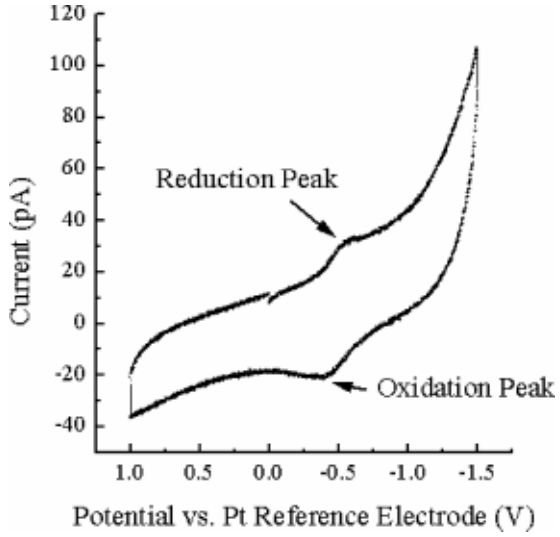

FIG. 7. Cyclic voltammetry data for a VACNF-based electrochemical probe device. These curves were taken in 1 mM ruthenium hexamine trichloride in a 0.1 M KCl solution using Pt reference and counter electrodes. The curves show clear oxidation and reduction peaks; the low level of measured faradic current indicates that only a small area of the device is electrochemically active, presumably the VACNF probe tip.

greater than 5 μm in diameter, were observed (refer to Fig. 6).

IV. ELECTROCHEMICAL CHARACTERIZATION

Electrochemical characterization of the probe devices was conducted using a CH Instruments Model 660A electrochemical analyzer workstation for cyclic voltammetry (CV). CV data was obtained by immersing the probes in a solution of 1 mM ruthenium hexammine trichloride (Polysciences, Inc., Warrington, PA) in a solution of 0.1 M KCl (Sigma, St. Louis, MO). Reference and counter electrodes were 20 mil Pt wires, polished with 0.05 μm aluminum oxide. Scan rates of 0.1 V/s were used over a maximum potential range of $+1$ V to -1.5 V. The potential placed on the VACNF was set at 0 V, where no redox activity occurred, for 5 s and then was swept to the negative minimum, reversed, and swept to the positive maximum, before returning to 0 V.

The CV data presented in Fig. 7 is representative of VACNF-based probe devices without any subsequent post-fabrication treatment, i.e., without any preparatory electrochemical or chemical modification. This data shows cathodic (reduction) and anodic (oxidation) peaks of ruthenium hexammine trichloride at -0.55 V and -0.45 V, respectively. Ruthenium hexammine trichloride has been documented as a highly reversible, single electron, outer sphere redox species, $Ru(NH_3)_6^{2+/3+}$, that is relatively insensitive to carbon surface functional groups or impurities.[9] The relative heights of the anodic and cathodic peaks indicate the reversibility of this reaction on our native carbon nanofiber electrode. The peaks also deviate from the sigmoidal shape expected from a microelectrode where the diffusional field of analyte is normally dominated by time-independent radial diffusion to the electrode surface.[10] This can be attributed to sluggish electron kinetics at the electrode surface, and the time scale of the experiment (scan rate).

The total diffusion-limited current to a spherical microelectrode is described by a time-dependent planar and time-independent radial term

$$i(t)=i_{\text{planar}}(t)+i_{\text{radial}}=\frac{nFADC}{\sqrt{\pi Dt}}+\frac{nFADC}{r},$$

where i is the anodic or cathodic peak current and is measured based on the peak height of the current with respect to the underlying capacitive (or charging) current due to the potential sweep ($i_{\text{peak cathodic}}=7.2$ pA), n is the number of electrons transferred in the redox process ($n=1$ for ruthenium hexammine trichloride), F is Faraday's number (95600 C/mole), A is the electrochemically active area of the electrode, D is the diffusion coefficient of the analyte[11] (6.3×10^{-6} cm^2/sec in 0.1 M KCl), C is the analyte concentration (1 mM), and t is the electrolysis time. For large values of Dt/r^2, the time-dependent term vanishes, and the equation reduces to

$$i=arnFDC,$$

where $a=2\pi$ for hemispherical electrodes.

Evaluation of these equations to determine the electrode radius indicates a radius of approximately 20 nm, which is consistent with dimensional measurements of the fabricated devices measured by electron microscopy.

V. CONCLUSION

In this work we have demonstrated the fabrication of high aspect ratio VACNF-based electrochemical probes. These devices were fabricated in a wafer-scale process that culminated in the realization of electrochemically active probe arrays. We have investigated the functionality of single probe devices by analyzing their response to a redox active compound (ruthenium hexammine trichloride) during cyclic

voltammetry. This data shows clear oxidation and reduction peaks with response that appears limited to an electrochemically active region at the probe tip. These probes are well suited for characterizing electrochemical phenomena with an unprecedented degree of spatial resolution. Expanding on the techniques demonstrated here, probe arrays limited only by the interconnect density could be fabricated offering massively parallel electrochemical sensing devices. These could be used for characterizing intracellular phenomena as well as providing parallel sensing elements for scanning electrochemical probes. This process is currently limited to being a research technique due to its dependence on EBL for definition of the VACNF catalyst sites. However, the advent of higher resolution conventional photolithographic techniques and high-throughput post-optical patterning technologies (nanoimprint, extreme ultraviolet, electron projection, etc.) should make it possible to turn this process into a large scale production technology.

ACKNOWLEDGMENTS

The authors wish to thank T. D. Chung for assistance with electrochemical evaluations, S. C. Jacobsen and C. T. Culbertson for helpful discussions, G. J. Bordonaro for assistance with photolithography and P. Fleming for assistance in sample preparation. This work was supported by the Laboratory-Directed Research and Development funding program of the Oak Ridge National Laboratory (ORNL). ORNL is managed for the Department of Energy by UT-Battelle, LLC under Contract No. DE-AC05-00OR22725. This work was performed in part at the Cornell Nanofabrication Facility (a member of the National Nanofabrication Users Network) which is supported by the National Science Foundation under Grant ECS-9731293, its users, Cornell University, and industrial affiliates.

[1] R. W. Wightman, J. A. Jankowski, R. T. Kennedy, K. T. Kawagoe, T. J. Schroeder, D. J. Leszczyszyn, J. A. Near, E. J. Diliberto, and O. H. Viveros, Proc. Natl. Acad. Sci. U.S.A. **88**, 10754 (1991).
[2] G. Alvarez de Toledo, R. Fernandez-Chacon, and J. M. Fernandez, Nature (London) **363**, 554 (1993).
[3] Y. Y. Lau, T. Abe, and A. G. Ewing, Anal. Chem. **64**, 1702 (1992).
[4] H. Lu and M. Gratzl, Anal. Chem. **71**, 2821 (1999).
[5] V. I. Merkulov, D. H. Lowndes, Y. Y. Wei, G. Eres, and E. Voekl, Appl. Phys. Lett. **76**, 3555 (2000).
[6] M. A. Guillorn, M. L. Simpson, G. J. Bordonaro, V. I. Merkulov, L. R. Baylor, and D. H. Lowndes, J. Vac. Sci. Technol. B **19**, 573 (2001).
[7] M. A. Guillorn, E. D. Ellis, M. L. Simpson, A. V. Melechko, V. I. Merkulov, G. J. Bordonaro, L. R. Baylor, and D. H. Lowndes, J. Vac. Sci. Technol. B **19**, 2598 (2001).
[8] V. I. Merkulov, M. A. Guillorn, D. H. Lowndes, M. L. Simpson, and E. Voelkl, Appl. Phys. Lett. **79**, 1178 (2001).
[9] P. Chen, M. A. Fryling, and R. L. McCreery, Anal. Chem. **67**, 3115 (1995).
[10] J. Wang, *Analytical Electrochemistry* (Wiley, New York, 2000).
[11] A. J. Bard and L. R. Faulkner, *Electrochemical Methods: Fundamentals and Applications, Second Edition* (Wiley, New York, 2001).